RM L55K30

NACA

RESEARCH MEMORANDUM

INVESTIGATION TO DETERMINE EFFECTS OF CENTER-OF-GRAVITY LOCATION ON THE TRANSONIC FLUTTER CHARACTERISTICS OF A 45° SWEPTBACK WING

By George W. Jones, Jr., and John R. Unangst

Langley Aeronautical Laboratory
Langley Field, Va.

NATIONAL ADVISORY COMMITTEE FOR AERONAUTICS

WASHINGTON
February 20, 1956
Declassified March 13, 1959

NATIONAL ADVISORY COMMITTEE FOR AERONAUTICS

RESEARCH MEMORANDUM

INVESTIGATION TO DETERMINE EFFECTS OF CENTER-OF-GRAVITY LOCATION ON THE TRANSONIC FLUTTER CHARACTERISTICS OF A 45° SWEPTBACK WING

By George W. Jones, Jr., and John R. Unangst

SUMMARY

An experimental investigation has been conducted in the 26-inch Langley transonic blowdown tunnel to determine effects of center-of-gravity location on the transonic flutter characteristics of a 45° sweptback-wing plan form of aspect ratio 4.0 and taper ratio 0.6. Solid-construction models of the plan form with streamwise NACA 65A004 airfoil sections and center-of-gravity locations at approximately 34 percent chord, 46 percent chord, and 58 percent chord, respectively, were fluttered at several Mach numbers between 0.8 and 1.35.

It was found that, for streamwise Mach numbers from 0.8 to 1.0, the variation with Mach number of the ratio of experimental flutter speed to a calculated incompressible flutter speed was not affected by center-of-gravity location. However, for Mach numbers from 1.0 to 1.35, there was an increase in flutter-speed ratio with Mach number which was different for each center-of-gravity position. Data from wings with successively more forward center-of-gravity locations showed successively larger values of flutter-speed ratio at Mach numbers from 1.0 to 1.35.

INTRODUCTION

As a result of several investigations in the 26-inch Langley transonic blowdown tunnel (refs. 1, 2, 3), extensive data have been obtained which give effects of plan form and Mach number on the flutter speed of swept wings in the transonic speed range. These data have been presented as the variation with plan form and Mach number of a ratio of the experimental flutter speed to a calculated, or reference, flutter speed based on two-dimensional, incompressible aerodynamic coefficients.

The question arose as to whether the flutter-speed ratios obtained in the previous investigations were functions only of Mach number and plan form or whether the ratios could be affected by changes in some of the elastic and inertia parameters which are present in the calculation of the reference flutter speed. A study of reference 4 suggested that, for the case of a given plan form having low values of the ratio of fundamental bending to torsion frequency, the parameter most likely to affect the variation of the flutter-speed ratio with Mach number was the chordwise location of the center of gravity. An investigation was made, therefore, in the 26-inch Langley transonic blowdown tunnel to determine the effect of the chordwise center-of-gravity location on the variation of the flutter-speed ratio with Mach number.

The plan form used in the investigation had an aspect ratio of 4, sweepback angle of the quarter-chord line of 45°, and a taper ratio of 0.6; and the centers of gravity were located at 34 and 58 percent chord. Results from references 2 and 3 were also available for the same plan form with the center of gravity located at 46 percent chord.

The trends shown by the results of this investigation have been previously discussed and analyzed in reference 5. The flutter-speed ratio at supersonic Mach numbers was shown to be a function of the chordwise center-of-gravity location and a method of analysis was developed therein which credibly explained the effect of the chordwise center-of-gravity location on the flutter-speed ratio.

The purpose of the present report is to present certain details of the center-of-gravity investigation which were not included in reference 5, namely the physical properties of the models used, the values of the test parameters at flutter, and the results of the flutter calculations. For completeness of the present report some of the information from reference 5 is repeated herein.

SYMBOLS

A aspect ratio including body intercept, $\dfrac{\text{Span}^2}{\text{Area}}$

a distance in wing semichords from midchord to elastic-axis position; taken perpendicular to quarter-chord line, positive rearward, $2x_o - 1$

A_g geometric aspect ratio, $\dfrac{(\text{Exposed span})^2}{\text{Exposed area}}$

b half-chord perpendicular to quarter-chord line, ft

b_r half-chord perpendicular to quarter-chord line at intersection of quarter-chord line and wing root, ft

b_s half-chord measured streamwise at intersection of wing root and fuselage, ft

c wing chord perpendicular to quarter-chord line, ft

f_{h_i} measured coupled bending frequencies, cps ($i = 1$ or 2)

f_t measured first coupled torsion frequency, cps

f_α uncoupled first torsion natural frequency relative to elastic axis, cps $f_\alpha = f_t\left[1 - \dfrac{\left(\dfrac{x_\alpha}{r_\alpha}\right)^2}{1 - \left(\dfrac{f_{h_1}}{f_t}\right)^2}\right]^{1/2}$

EI bending stiffness, lb/in^2

GJ torsion stiffness, lb/in^2

g_h structural damping coefficient in bending

I_α mass moment of inertia of wing section about elastic axis, $slug\text{-}ft^2/ft$

l length of wing panels outside fuselage, measured along quarter-chord line, ft

M Mach number

m mass of wing per unit length along quarter-chord line, slugs/ft

q dynamic pressure, lb/sq ft

r_α nondimensional radius of gyration of wing section about elastic axis, $\left(I_\alpha/mb^2\right)^{1/2}$

V airstream velocity, ft/sec

V_n component of stream velocity normal to quarter-chord line, ft/sec

V_e/V_R flutter-speed ratio, ratio of experimental flutter speed to a calculated reference flutter speed

x_o distance, perpendicular to quarter-chord line, of elastic axis of wing section behind leading edge, fraction of chord

x_{cg} center-of-gravity location, fraction of chord behind leading edge, measured perpendicular to quarter-chord line

x_α distance in semichords (measured perpendicular to quarter-chord line) from wing elastic axis to wing center of gravity, positive when center of gravity is behind the elastic axis

η nondimensional coordinate along quarter-chord line, fraction of length l

μ mass-ratio parameter, $m/\pi\rho b^2$ (values given in table II taken at 0.75η)

λ taper ratio, Tip chord/Chord in plane of symmetry

Λ angle of sweepback of quarter-chord line, deg

ρ air density, slugs/cu ft

ω angular frequency of vibration, radians/sec

ω_{h_i} angular bending frequency, radians/sec $(2\pi f_{h_i})$

ω_α angular uncoupled torsion frequency, radians/sec $(2\pi f_\alpha)$

Subscripts:

e experimental values

R calculated values

MODELS

Model Geometry

The plan form selected for these tests had an aspect ratio of 4, a quarter-chord sweepback angle of 45°, and a taper ratio of 0.6. Models of the plan form had NACA 65A004 airfoil sections along streamwise chords, a wing span of 1.142 feet, and the ratio of sting diameter to wing span was 0.22.

Two types of models of this plan form were constructed. One type had the center of gravity located at approximately 34 percent chord while the other type had the center of gravity located at approximately 58 percent chord (measurements perpendicular to the quarter-chord line). The models of reference 3, for which data are presented herein for comparison (see table I(b)), had a center-of-gravity location at approximately 46 percent chord. The center-of-gravity locations measured in percent of streamwise chord were 37 percent, 49 percent, and 61 percent. Because of their destruction by flutter, several models of each type were necessary in order to obtain the desired data.

Model Materials and Construction

Figure 1 gives a plan-form view of the three types of models cut away to show the construction details. The models with a center of gravity at 34 percent chord were made with a Compreg (laminated, compressed, resin-impregnated maple) core. These models had a lead-bismuth-tin mixture leading edge (50 percent lead, 25 percent bismuth, 25 percent tin by weight) and an outer wrapping of a 0.003-inch-thick Fiberglas cloth. The models with a center-of-gravity position at 58 percent chord were also made with a Compreg core and had a lead-bismuth-tin mixture trailing edge and a Fiberglas wrap. The Fiberglas wrap for the models with 58-percent center-of-gravity location was of three layers; two layers were unilateral Fiberglas cloth (majority of strength in one direction similar to wood grain) with strength directions forming 45° diagonals across the quarter-chord line and the third layer was an outer wrap of 0.003-inch Fiberglas cloth. The lead-bismuth-tin mixture used for leading or trailing edges, was cut perpendicular to the quarter-chord line at 1/2-inch spanwise intervals to minimize the effect on wing stiffness. The models of reference 3 which had the same plan form as the models of this report but a location of the center of gravity at 46 percent chord were of solid Compreg wrapped with two layers of 0.003-inch Fiberglas cloth, except for one model of plain Compreg with no wrap. On all models the layers of Fiberglas cloth were bonded to each other and to the core with Paraplex cement. The Fiberglas wrapping extended into the wing mounting block at the root for approximately 1/4 inch. The 3/8-inch-thick wing mounting block was an integral part of the wing core of Compreg wood (see fig. 1) and fitted flush in a slot in the sting mount.

Model Physical Parameters

Measurements were made of the following physical parameters on each wing panel of every model tested: (1) elastic-axis position, (2) first and second bending and first torsion coupled natural frequencies, and (3) structural damping coefficient in bending. Measurements were made of the following parameters on at least one wing panel of each type of model constructed: spanwise variation of mass, center-of-gravity location, and mass moment of inertia about the elastic axis (see table I). Measurements made of the spanwise variation of bending and torsion stiffness EI and GJ for a representative panel of each type of model are presented in figure 2. A discussion of the methods used to measure the various physical properties may be found in references 2, 3, and 6.

APPARATUS AND TESTS

The tests were made in the 26-inch Langley transonic blowdown tunnel. A desirable flutter-test feature of this tunnel is that during its operation a selected Mach number which is controlled by an orifice plate can be held approximately constant (after the orifice is choked) while test section stagnation pressure (and thus density) is varied. The tunnel can be operated through the subsonic Mach numbers and up to a supersonic Mach number of approximately 1.45 and the tunnel density range is from approximately 0.001 to 0.012 slug per cubic foot. A more complete description of the tunnel may be found in reference 3.

The flutter-model wings were mounted at 0° angle of attack on a cylindrical sting fuselage. This sting extends into the subsonic flow region of the tunnel and thereby eliminates the formation of a bow shock wave which might reflect from the tunnel walls onto the model. The fundamental frequency of the support system is approximately 15 cycles per second.

Both wing panels of each model were instrumented with wire strain gages. A recording oscillograph was used to give a simultaneous record of the strain-gage signals, tunnel stagnation temperature and pressure, and test-section static pressure. The strain-gage signals were used to indicate the start of flutter and the frequency of wing oscillations.

The tests were conducted in such a manner that the flutter speed and flutter frequency were determined on each model for several Mach numbers throughout the transonic range from about $M = 0.8$ to about $M = 1.4$. A more detailed discussion of the testing technique as well as the model support system and the instrumentation may be found in reference 3.

RESULTS

Method of Analysis

The results of the present tests are presented as the variation with Mach number of a ratio of the experimental flutter speed to a calculated, or reference, flutter speed. The reference flutter speeds for these test results were calculated (as in ref. 3) by use of two-dimensional, incompressible air forces combined with cantilever beam deflection modes in a Rayleigh-type analysis. In the analysis, the mode shape of the wings during flutter was represented by the nondimensional shapes of the first two uncoupled bending modes and the first uncoupled torsion mode of a uniform cantilever beam. The frequencies used in the analysis were the measured values of the first two bending natural frequencies (these values were assumed to approximate the uncoupled values) and the uncoupled value of the first torsion frequency (which was obtained from the measured coupled value by the approximate formula given in the list of symbols herein).

General Comments

Certain general comments made in the section entitled "Results" of reference 3 concerning the nature of flutter encountered and the effects of testing technique apply to the present tests, and may be summarized briefly by the following statements:

(1) The flutter observed in the tests was of the classical bending-torsion type.

(2) The amplitude of wing oscillations following the start of flutter did not continually increase with time but increased rapidly to some nearly constant value.

(3) An easily defined start of flutter was not always obtained. Often, a period of intermittent sinusoidal-type oscillations in both bending and torsion (designated a low-damping region) preceded continuous flutter. In such cases, the exact start of flutter was difficult to pick on the oscillograph record. These cases are treated in the same manner as similar cases in reference 3. Briefly, this involves selecting two data points for those cases in which the exact start of flutter could not be determined. The first point is taken near the beginning of the intermittent sinusoidal-type oscillations and is designated as the start of a low-damping period. The second point is taken near the beginning of continuous flutter and is designated as a point of flutter.

(4) In some cases, the two panels of the same model did not flutter simultaneously; probably because of slight differences in physical properties between wing panels. In such cases, separate flutter points are presented for the start of flutter for each panel.

(5) The operating characteristics of the tunnel were such that frequently during a single run (a run is defined as one operation of the tunnel from valve opening to valve closing) the tunnel-operating curve of dynamic pressure as a function of Mach number intersected the wing flutter-boundary curve of dynamic pressure required for flutter against Mach number at more than one point. In such cases, each point of intersection is presented in the data.

Presentation of Data

The results of the investigation are tabulated in table II as are some data of reference 3 (table II(b)). The first five columns of the table contain a brief description of the chronological behavior of each wing panel during each run. The first column gives the identification number of the model. A model designation of reference 2 in this column indicates that the data for the run were taken from reference 2 in which no record was kept of the numbers of individual, similarly constructed models of the same plan form. The second column gives the run number, and the third column shows in chronological order the data points which occurred during each run. The fourth and fifth columns contain code letters which describe the behavior of each wing panel at the time of each data point. The code letters and their designations are as follows:

F flutter

D low damping

E end of flutter with dynamic pressure increasing

N no flutter

G strain gages inoperative, no record

X panel destroyed or not installed

Subscripts 1 or 2 attached to these letters indicate the phenomena are related to the first or second occurrence of flutter on the panel during the given run. For example, a series of data points obtained during a given run might be coded as follows:

Run	Point	Wing behavior	
		Left	Right
3	1	F_1	F_1
	2	E_1	E_1
	3	D_2	D_2
	4	F_2	D_2
	5	F_2	F_2

In this example, five data points were obtained during run 3. At the time of point 1, both panels began to flutter and continued to flutter until point 2 when both panels stopped fluttering although the tunnel dynamic pressure was increasing. Then, near the time of point 3 both panels began sinusoidal-type oscillations, designated as low damping, prior to a second occurrence of flutter which became continuous on the left panel near the time of point 4. The right panel continued to exhibit low-damping behavior until point 5 when it too began a continuous flutter for the second time during run 3.

Figures 3 through 6 present the results of the investigation in the form of plots of the ratio of experimental to reference flutter speed V_e/V_R as a function of Mach number. Figures 3, 4, and 5 each present the flutter-speed ratios obtained at various transonic Mach numbers on models having one of the three center-of-gravity positions investigated (fig. 4 is data from ref. 3). In these figures, the low-damping periods are indicated by dashed lines beginning at the point selected at the start of the low-damping period and extending to the point of continuous flutter. The data point near the beginning of a low-damping period is denoted by the lower end of the dashed line whereas the data point near the beginning of continuous flutter is marked by a symbol. The path of the dashed lines is a function of tunnel operating conditions as the flutter point was approached. The points at the start of flutter are indicated by plain symbols and points at the end of flutter are indicated by shaded symbols. Figure 6 is a plot which superimposes the three faired flutter boundaries of figures 3, 4, and 5.

DISCUSSION

As may be observed in figure 6, the flutter-speed ratios for the three center-of-gravity positions merged in the high subsonic range ($0.8 \leqq M_e \leqq 1.0$) with values near 1.0. Thus, in the high subsonic range, the reference flutter speed accurately predicts the experimental flutter speed. In the low supersonic range ($1.0 \leqq M_e \leqq 1.35$), there is a rapid increase in V_e/V_R as the Mach number increases, but the rate of increase is different for the various center-of-gravity positions so that each configuration has a separate flutter boundary. Examination of figure 6 shows that the rate of increase of V_e/V_R with Mach number becomes larger as the center of gravity moves forward. Thus, for the test plan form in the supersonic speed range investigated, the flutter-speed ratio is not a function of plan form and Mach number alone but also appears to be a function of center-of-gravity position.

Some doubt may be expressed that the difference in the V_e/V_R curves in figure 6 should be attributed to chordwise changes in center-of-gravity location because, as previously stated, models of the present investigation which had different center-of-gravity locations also had different values of the elastic and inertia parameters ω_h/ω_α, r_α, m, and a. It can not be proved from the available data that the differences in the V_e/V_R curves were not affected by the changes in these other parameters. However, on the basis of the analysis in reference 5 which uses trends and conclusions drawn in reference 4, the chordwise center-of-gravity location would appear to be the major factor in accounting for the present differences in the supersonic values of the flutter-speed ratios.

The flutter data as presented in figure 6 cannot indicate directly the relative flutter susceptibility of a given wing design as the center of gravity is moved, since both V_e and V_R would be expected to change. However, it can be shown with the aid of a comparison of the sharp upsweep of the curve of V_e/V_R for the 34 percent chord center-of-gravity location with the more gentle upsweep of the curves for the 46- and 58-percent-chord locations that it may be possible to reduce the severity of the flutter problem at supersonic speeds by a suitable forward location of the center of gravity.

In the subsonic speed range the curves of V_e/V_R in figure 6 are the same for all center-of-gravity locations tested and thus do not reveal the fact that the actual flutter speeds vary with the center-of-gravity location. Nor can the effects of center-of-gravity location on the flutter speed be obtained by directly comparing the experimental flutter speeds because the models constructed with different center-of-gravity locations had necessary differences in mass and stiffness parameters which affect the flutter speed. However, an examination of the nondimensional flutter-speed coefficient $V_R/b_r\omega_\alpha$ given in table II shows that, for equal values of mass ratio, the flutter-speed coefficients at subsonic speeds had approximately a 25-percent increase as the center of gravity shifted from 0.58 chord to 0.46 chord and an additional increase of approximately 75 percent as the center of gravity shifted from 0.46 chord to 0.34 chord. These increases in $V_R/b_r\omega_\alpha$, which were based on three-dimensional calculations to the extent that spanwise variations of mass, geometry, and airfoil vibration mode shape were taken into account, are similar to those shown by the calculations of reference 4 for a two-dimensional wing.

CONCLUSIONS

The conclusions drawn from an experimental investigation of effects of center-of-gravity location on the transonic flutter characteristics of a 45° sweptback wing follow:

1. For streamwise Mach numbers from 1.0 to 1.35, the flutter-speed ratio was affected by center-of-gravity changes. In this Mach number range, there was an increase in flutter-speed ratio (ratio of experimental to calculated flutter speeds) with Mach number which was different for each center-of-gravity position. The rate of this increase in flutter-speed ratio became larger as the center of gravity moved forward.

2. For streamwise Mach numbers from 0.8 to 1.0, presenting the results as a flutter-speed ratio removed the effect of center-of-gravity position since the flutter-speed ratio was approximately 1.0 in this range for all center-of-gravity positions tested.

3. The calculated flutter-speed coefficients for equal values of mass density ratio, increased approximately 25 percent when the center of gravity was changed from 0.58 chord to 0.45 chord and increased approximately an additional 75 percent when the center of gravity was changed from 0.45 chord to 0.34 chord.

Langley Aeronautical Laboratory,
National Advisory Committee for Aeronautics,
Langley Field, Va., October 15, 1955.

REFERENCES

1. Bursnall, William J.: Initial Flutter Tests in the Langley Transonic Blowdown Tunnel and Comparison With Free-Flight Flutter Results. NACA RM L52K14, 1953.

2. Jones, George W., Jr., and DuBose, Hugh C.: Investigation of Wing Flutter at Transonic Speeds for Six Systematically Varied Wing Plan Forms. NACA RM L53G10a, 1953.

3. Unangst, John R., and Jones, George W., Jr.: Some Effects of Sweep and Aspect Ratio on the Transonic Flutter Characteristics of a Series of Thin Cantilever Wings Having a Taper Ratio of 0.6. NACA RM L55I13a, 1955.

4. Theodorsen, Theodore, and Garrick, I. E.: Mechanism of Flutter - A Theoretical and Experimental Investigation of the Flutter Problem. NACA Rep. 685, 1940.

5. Loftin, Laurence K., Jr.: Flutter Characteristics of Swept Wings at Transonic Speeds. NACA RM L55E19a, 1955.

6. Land, Norman S., and Abbott, Frank T., Jr.: Transonic-Flutter Investigation of a Fighter-Airplane Wing Model and Comparison With a Systematic Plan-Form Series. NACA RM L55B16, 1955.

TABLE I.- PHYSICAL PROPERTIES OF MODELS

(a) Wings with center of gravity at approximately 34 percent chord

Parameter	Wings 1, 2, 3, 4, and 5
NACA section	65A004
A	4
Λ, deg	45
λ	0.6
Panel λ	0.657
Span, ft	1.142
A_g	1.65
l, ft	0.630
b_r, ft	0.123
b_s, ft	0.163
Average $x_{c.g.}$	0.337
g_h	0.0214

η	Wing No. 5 (left panel)			
	x_α	a	r_α^2	m, slugs/ft
0.05	−0.305	0.028	0.465	0.00899
.15	−.321	.035	.457	.00869
.25	−.337	.041	.450	.00835
.35	−.352	.047	.442	.00793
.45	−.368	.054	.441	.00737
.55	−.383	.060	.487	.00625
.65	−.398	.067	.504	.00568
.75	−.414	.074	.513	.00518
.85	−.429	.081	.516	.00475
.95	−.444	.087	.515	.00433

Frequency	Wing No. 1		Wing No. 2		Wing No. 3		Wing No. 4		Wing No. 5	
	Left Panel	Right panel	Left panel	Right panel	Left panel	Right panel	Left panel	Right panel	Left panel	Right panel
f_{h_1}	61	61	61	60	60	65	64	61	61	61
f_{h_2}	332	322	342	327	322	361	341	322	318	331
f_{t_1}	210	208	226	230	232	228	227	213	217	218
f_{α_1}	173.2	172.4	187	191	192	188	188	176	179.3	180
$(\omega_{h_1}/\omega_{\alpha_1})^2$	0.1240	0.1252	0.1062	0.0995	0.0977	0.1172	0.1163	0.1200	0.1150	0.1146
$(\omega_{h_2}/\omega_{\alpha_1})^2$	3.6743	3.4885	3.3484	2.9465	2.8126	3.6716	3.3005	3.3663	3.1455	3.3740

TABLE I.- Continued

(b) Wings with center of gravity at approximately 46 percent chord

Parameter	Wing of Ref. 2 Wings 1 and 2
NACA section	65A004
A	4
Λ, deg	45
Panel λ	0.657
Span, ft	1.142
A_g	1.65
l, ft	0.630
b_r, ft	0.123
b_s, ft	0.163
Average x_{cg}	0.455
g_h	0.030

η	Wing of Ref. 2				Wing no. 1			
	x_α	a	r_α^2	m, slugs/ft	x_α	a	r_α^2	m, slugs/ft
0.05	-0.02	-0.07	0.22	0.00561	0.037	-0.117	0.233	0.00733
.15	.01	-.10	.22	.00527	.030	-.110	.234	.00648
.25	.04	-.10	.23	.00493	.023	-.102	.235	.00576
.35	.07	-.15	.24	.00458	.016	-.095	.236	.00516
.45	.09	-.18	.24	.00424	.009	-.088	.237	.00472
.55	.12	-.21	.25	.00389	.002	-.082	.238	.00435
.65	.15	-.24	.26	.00355	-.005	-.074	.239	.00407
.75	.17	-.26	.26	.00321	-.012	-.067	.240	.00382
.85	.20	-.29	.27	.00286	-.018	-.060	.241	.00361
.95	.23	-.32	.28	.00252	-.025	-.053	.242	.00343

Frequency	Wing of Ref. 2	Wing No. 1		Wing No. 2	
	Both panels	Left panel	Right panel	Left panel	Right panel
f_{h_1}	88	67	64	78	73
f_{h_2}	462	357	367	399	387
f_{t_1}	370	356	342	389	378
f_{α_1}	361	356	342	389	378
$(\omega_{h_1}/\omega_{\alpha_1})^2$	0.0594	0.0354	0.0350	0.0402	0.0373
$(\omega_{h_2}/\omega_{\alpha_1})^2$	1.638	1.006	1.151	1.053	1.049

TABLE I.- CONCLUDED

(c) Wings with center of gravity at approximately 58 percent chord

Parameter	Wings 1, 2, 3, 4, and 5
NACA section	65A004
A	4
Λ, deg	45
λ	0.6
Panel λ	0.657
Span, ft	1.142
A_g	1.65
l, ft	0.630
b_r, ft	0.123
b_s, ft	0.163
Average x_{cg}	0.5795
g_h	0.0327

η	Wing No. 3 (right panel)			
	x_α	a	r_α^2	m, slugs/ft
0.05	0.061	0.099	0.226	0.01176
.15	.074	.086	.241	.01161
.25	.086	.074	.252	.01093
.35	.098	.062	.259	.01040
.45	.111	.049	.260	.00951
.55	.123	.036	.255	.00818
.65	.135	.024	.258	.00732
.75	.148	.011	.273	.00660
.85	.160	-.001	.284	.00598
.95	.173	-.013	.389	.00540

Frequency	Wing No. 1		Wing No. 2		Wing No. 3		Wing No. 4		Wing No. 5	
	Left panel	Right panel	Left panel	Right panel	Left panel	Right panel	Left panel	Right panel	Left panel	Right panel
f_{h_1}	48	51	50	50	49	51	52	51	52	51
f_{h_2}	245	255	247	247	230	235	238	236	226	230
f_{t_1}	382	382	385	385	380	383	391	386	363	360
f_{α_1}	371.6	371.6	374.6	374.6	370	373	380	376	353	350
$(\omega_{h_1}/\omega_{\alpha_1})^2$	0.01668	0.01883	0.01781	0.01781	0.01764	0.01888	0.01833	0.01808	0.02129	0.02104
$(\omega_{h_2}/\omega_{\alpha_1})^2$	0.4347	0.4709	0.3437	0.3437	0.3870	0.3878	0.3914	0.3949	0.40965	0.4313

TABLE II.- COMPILATION OF ANALYTICAL AND EXPERIMENTAL RESULTS

Wing panel behavior code: F - flutter; E - end of flutter (dynamic pressure increasing); N - no flutter; G - strain gages not working; D - low damping; X - wing panel destroyed or not installed

Subscripts: 1 - associated with first occurrence of flutter during the run; 2 - associated with second occurrence of flutter during the run

(a) Wings with center of gravity at approximately 34 percent chord

Model	Run*	Point**	Wing Behavior Left	Wing Behavior Right	M_e	V_e/V_R	ρ_e slugs/cu ft	μ_e	$\sqrt{\mu_e}$	ω_α radians/sec	ω_h/ω_α	ω_e radians/sec	ω_e/ω_α	V_e ft/sec	V_R ft/sec	$V_e/b_r\omega_\alpha$	$V_R/b_r\omega_\alpha$	q_e lb/ft²
1	1	1	F_1	F_1	0.836	1.146	0.0034	58.11	7.62	1083.2	0.6713	772.8	1.063	885.5	772.6	6.646	5.80	1333
1	2	1	F_1	F_1	.890	1.017	.0022	89.80	9.48	1083.2	.6399	628.3	.907	933.7	917.7	7.008	6.89	959
1		2	F_1	E_1	.995	1.101	.0021	94.08	9.70	1078.2	.6362	—	—	1025	930.9	7.729	7.02	1103.2
1		3	E_1	F	1.049	1.147	.0021	94.08	9.70	1083.2	.6362	647.2	.939	1072.4	935.1	8.049	7.02	1207.5
1	3	1	F_1	F_1	.903	1.054	.0023	85.90	9.27	1083.2	.6435	—	—	950.8	901.8	7.136	6.77	1039.6
1		2	E_1	E_1	1.064	1.228	.0023	85.90	9.27	1083.2	.6435	—	—	1107.6	901.8	8.313	6.77	1410.8
1	4	1	F_1	F_1	.925	1.075	.0024	82.32	9.07	1083.2	.6468	634.6	.906	953.8	887.1	7.159	6.66	1091.7
1		2	G	E_1	.963	1.101	.0024	82.32	9.07	1083.2	.6468	—	—	977.1	887.1	7.334	6.66	1145.7
1	5	1	G	F_1	.916	1.099	.0025	79.02	8.89	1083.2	.6498	647.2	.919	958.5	872.5	7.194	6.55	1102.5
1	6	1	G	F_1	.899	1.066	.0024	82.32	9.07	1083.2	.6468	647.2	.924	945.9	887.1	7.110	6.66	1073.7
2	7	1	F_1	F_1	.934	.997	.0022	89.80	9.48	1185.6	.6398	672	.886	1000.7	1003.3	6.862	6.88	1101.5
2		2	E_1	E_1	1.124	1.161	.0022	89.80	9.48	1185.6	.6398	—	—	1164.6	1003.3	7.986	6.88	1491.9
2	8	1	F_1	F_1	.936	1.010	.0023	85.90	9.27	1185.6	.6434	679	.890	997.5	987.3	6.840	6.77	1144.3
2		2	E_1	E_1	1.099	1.057	.0023	85.90	9.27	1185.6	.6434	—	—	1142.4	987.3	7.834	6.77	1500.8
3	9	1	F_1	F_1	.843	.929	.0024	82.32	9.07	1195.1	.6468	766	.991	909.9	979	6.190	6.66	993.5
3		2	E_1	E_1	1.072	1.175	.0026	75.98	8.72	1195.1	.6527	—	—	1113.9	948.1	7.578	6.45	1613
3		3	D_2	G	1.147	1.440	.0040	49.39	7.03	1195.1	.6813	—	—	1153.4	801.1	7.846	5.45	2660.7
3		4	F_2	G	1.148	1.487	.0044	44.90	6.70	1195.1	.6869	1024	1.247	1150	773.2	7.823	5.26	2909.5
3	10	1	F_1	X	.968	1.059	.0025	79.02	8.89	1206.4	.6498	760	.970	1028.9	971.9	6.934	6.55	1323.3
3		2	E_1	X	1.063	1.147	.0025	79.02	8.89	1206.4	.6498	—	—	1114.8	971.9	7.513	6.55	1553.5
3		3	F_2	X	1.145	1.495	.0045	43.90	6.63	1206.4	.6680	1005	1.211	1158.3	774.6	7.806	5.22	3018.7
3	11	1	F_1	X	.951	1.026	.0024	82.32	9.07	1206.4	.6468	729	.934	1013.6	988.3	6.831	6.66	1232.9
3		2	F_1	X	1.063	1.160	.0026	75.98	8.72	1206.4	.6527	—	—	1110.4	957.1	7.483	6.45	1602.9
3		3	F_2	X	1.141	1.437	.0040	49.39	7.03	1206.4	.6813	966	1.200	1162.5	808.7	7.834	5.45	2702.8
4	12	1	F_1	F_1	.984	1.055	.0024	82.32	9.07	1141.0	.6468	767	1.039	986.5	934.7	7.089	6.66	1167.8
4		2	E_1	E_1	1.075	1.254	.0027	73.17	8.55	1141.0	.6595	—	—	1117.7	891.2	7.964	6.35	1686.5
4		3	F_2	D_2	1.097	1.362	.0033	59.87	7.74	1141.0	.6694	949	1.243	1121.8	823.8	7.993	5.87	2076.4
4		4	F_2	F_2	1.085	1.379	.0035	56.45	7.51	1141.0	.6732	930	1.211	1110.5	805.6	7.913	5.74	2145.8
4	13	1	F_1	F_1	.825	1.028	.0030	65.85	8.12	1141.0	.6626	754	.997	878.4	854.7	6.259	6.09	1157.4
4	14	1	F_1	F_1	.875	1.044	.0027	73.17	8.55	1141.0	.6595	761	.991	930.7	891.2	6.632	6.35	1169.4
4	15	1	F_1	F_1	.891	1.043	.0025	79.02	8.89	1141.0	.6498	744	1.004	958.6	919.2	6.830	6.55	1148.6
4	16	1	G	F_1	.908	1.023	.0023	85.90	9.27	1141.0	.6434	729	.993	971.8	950.1	6.925	6.77	1086.1
5	17	1	F_1	F_1	.936	1.049	.0022	89.80	9.48	1129.7	.6398	707	.978	1002.5	956.0	7.215	6.88	1105.5
5		2	E_1	E_1	1.128	1.222	.0022	89.80	9.48	1129.7	.6398	—	—	1167.9	956	8.405	6.88	1500.4
5	18	1	F_1	F_1	.875	1.007	.0023	85.90	9.27	1129.7	.6434	672	.925	947.1	940.7	6.816	6.77	1011.5
5		2	E_1	E_1	1.053	1.199	.0024	82.32	9.07	1129.7	.6468	—	—	1110.1	925.4	7.989	6.66	1478.8

* Run - A run is defined as one operation of the blowdown tunnel from valve opening to valve closing.

** Point - Chronological order in which recorded points occurred during the test run.

TABLE II.- Continued

(b) Wings with center of-gravity position at approximately 46-percent

Model	Run	Point	Wing Behavior Left	Wing Behavior Right	M_e	V_e/V_R	ρ_e slugs/cu ft	μ_e	$\sqrt{\mu_e}$	ω_α radians/sec	ω_R/ω_α	ω_R radians/sec	ω_e radians/sec	ω_e/ω_R	V_e ft/sec	V_R ft/sec	$V_e/b_r\omega_\alpha$	$V_R/b_r\omega_\alpha$	q_e lb/ft^2
(Ref.2)	1	1	F_1	F_1	0.813	1.032	0.0033	37.10	6.09	2268	0.5295	1201.5	1047	0.871	805.4	780.4	2.88	2.80	1070
"	2	1	F_1	F_1	.797	1.039	.0031	39.49	6.28	2268	.5245	1200.9	1047	.872	795.6	765.8	2.85	2.75	961
"	3	1	F_1	F_1	.863	1.036	.0028	43.72	6.61	2268	.5160	1170.3	995	.850	856.0	825.8	3.06	2.96	1026
"	4	1	F_1	F_1	.863	1.030	.0028	43.72	6.61	2268	.5160	1170.3	—	—	850.7	825.8	3.04	2.96	1013
"	5	1	F_1	F_1	.906	1.047	.0026	47.08	6.86	2268	.5095	1155.5	995	.861	867.7	848.1	3.18	3.04	1024
"	6	1	F_1	F_1	.904	1.062	.0027	45.34	6.73	2268	.5128	1163	958	.824	888.8	837.0	3.19	3.00	1067
"	7	1	N	D_1	1.396	1.987	.0029	42.21	6.50	2268	.5192	1177.5	—	—	1396.7	817.4	4.65	2.92	2438.8
"		2	N	F_1	1.376	1.641	.0034	36.01	6.00	2268	.5322	1207	1585	1.313	1267.8	772.7	4.55	2.77	2732.4
"		3	D_1	F_1	1.326	1.800	.0048	25.50	5.05	2268	.5569	1263	—	—	1215	675.1	4.36	2.42	2066.7
"		4	F_1	F_1	1.340	1.830	.0054	22.67	4.76	2268	.5643	1279.8	1755	1.371	1214.8	663.9	4.36	2.38	3984.5
"	8	1	N	F_1	1.023	1.095	.0021	59.73	7.73	2268	.4870	1104.5	1119	1.013	1011	923	3.62	3.32	1073
"		2	N	F_2	1.361	1.614	.0033	36.88	6.07	2268	.5302	1202.4	1540	1.281	1256	778	4.50	2.79	2603
"	9	1	F_1	F_1	.975	1.124	.0024	51.23	7.16	2268	.5016	1137.6	1121	.985	981	873	3.51	3.13	1155
"		2	F_1	E_1	1.301	1.540	.0031	38.99	6.24	2268	.5255	1191.8	—	—	1224	795	4.38	2.84	2322
"	10	1	F_1	F_1	.975	1.125	.0025	49.77	7.05	2268	.5047	1144.6	1023	.894	973	865	3.48	3.10	1183
"	11	1	F_1	F_1	.944	1.052	.0026	47.08	6.86	2268	.5095	1155.5	1040	.900	921	875	3.30	3.04	1103
"	12	1	F_1	F_1	.794	.972	.0028	43.72	6.61	2268	.5160	1170.3	1063	.908	803.3	825.8	2.88	2.96	903
"		2	F_1	F_1	.924	1.020	.0027	45.34	6.73	2268	.5128	1163.0	1162	.999	854	837	3.06	3.00	984
"	13	1	N	F_1	.961	1.065	.0022	55.64	7.46	2268	.4938	1120	1096	.978	946	901.1	3.42	3.22	1005
"		2	N	F_2	1.342	1.600	.0035	34.98	5.92	2268	.5342	1212	1517	1.295	1223	764.4	4.38	2.74	2618
1	14	1	N	F_1	.940	1.059	.0018	80.93	9.00	2148.8	.4019	863.6	859	.995	977	922.4	3.69	3.49	860
1		2	N	E_1	1.039	1.129	.0017	85.69	9.26	2148.8	—	—	859	—	1062	940.9	4.01	3.56	942
1	15	1	N	F_1	.862	1.007	.0019	76.67	8.76	2148.8	.4078	876.3	856	.980	908	901.3	3.43	3.41	768
1		2	N	E_1	1.049	1.140	.0017	85.69	9.26	2148.8	—	—	856	—	1073	940.9	4.06	3.56	1004
1	16	1	F_1	F_1	.871	1.041	.0024	60.70	7.79	2195	.4325	949.3	919	.968	882	847.5	3.27	3.14	922
1		2	0	E_1	1.175	1.336	.0020	72.84	8.53	2148.8	—	—	919	—	1183	885.4	4.48	3.35	1486
1		3	0	D_2	1.293	1.705	.0037	39.37	6.27	2148.8	.4713	1012.7	—	—	1217	713.6	4.60	2.70	2753
1		4	0	F_2	1.292	1.741	.0038	38.34	6.19	2148.8	.4736	1017.7	1460	1.435	1233	707.3	4.66	2.68	2820
1	17	1	F_1	0	.830	1.044	.0026	56.03	7.49	2236.8	.4402	984.6	982	.997	879	841.9	3.19	3.06	996
2	18	1	D_1	0	1.348	1.643	.0041	35.53	5.96	2444.2	—	—	—	—	1289	784.7	4.29	2.61	3411
2		2	F_1	0	1.346	1.712	.0049	29.72	5.45	2444.2	.4925	1203.8	1591	1.322	1271	742.6	4.23	2.47	3979
2	19	1	D_1	0	1.219	1.423	.0033	44.15	6.64	2444.2	—	—	—	—	1202	844.8	4.00	2.81	2388
2		2	F_1	0	1.192	1.445	.0037	39.37	6.27	2444.2	.4712	1151.7	1302	1.130	1173	811.7	3.90	2.70	2537
2	20	1	D_1	0	1.204	1.411	.0033	44.15	6.64	2444.2	—	—	—	—	1192	844.8	3.96	2.81	2328
2		2	F_1	0	1.186	1.564	.0039	37.35	6.11	2444.2	.4756	1162.4	1353	1.164	1166	804.4	3.88	2.68	2628
2	21	1	F_1	0	.836	1.063	.0025	58.27	7.63	2444.2	.4369	1067.9	900	.843	997	929	3.32	3.09	1104
2	22	1	N	D_1	1.307	1.600	.0037	39.37	6.27	2375	.4713	1119.3	—	—	1262	788.8	4.32	2.70	2946
2		2	N	F_1	1.332	1.682	.0044	33.11	5.75	2375	.4848	1151.4	1539	1.337	1253.1	744.9	4.29	2.55	3454
2	23	1	F_1	F_1	.882	.980	.0022	66.22	8.14	2410	.4237	1021.1	905	.886	939.8	960	3.17	3.24	971
2		2	E_1	E_1	1.149	1.183	.0022	72.84	8.53	2410	—	—	—	—	1173.9	993	3.96	3.35	1378
2		3	N	D_2	1.285	1.528	.0033	44.15	6.64	2375	.4618	1096.8	—	—	1254	820.9	4.29	2.81	2595
2		4	N	F_2	1.283	1.591	.0038	38.34	6.19	2375	.4736	1124.8	1495	1.329	1245.8	782.9	4.26	2.68	2949
2	24	1	F_1	F_1	.854	1.037	.0028	52.03	7.21	2410	.4475	1078.5	955	.885	912.8	880	3.08	2.97	1166
2	25	1	F_1	F_1	.908	1.033	.0024	60.70	7.79	2410	.4346	1142.6	930	.892	961.3	931	3.24	3.14	1109
2		2	E_1	0	1.085	1.184	.0023	63.34	7.96	2410	—	—	—	—	1116.1	943	3.76	3.18	1432
2		3	D_2	0	1.142	1.242	.0026	56.03	7.49	2444.2	.4402	1075.9	—	—	1142.3	920	3.80	3.06	1696
2		4	F_2	0	1.176	1.306	.0028	52.03	7.21	2444.2	.4475	1093.8	1115	1.019	1166.4	892.9	3.88	2.97	1905
2	26	1	F_1	0	.874	.997	.0025	58.27	7.63	2444.2	.4367	1067.4	892	.836	926.3	929	2.08	3.09	1072
2	27	1	F_1	0	.920	.954	.0022	66.22	8.14	2444.2	.4236	1035.4	817	.789	967.7	974.1	3.22	3.24	1030
2		2	E_1	0	1.055	1.097	.0021	69.37	8.33	2444.2	—	—	—	—	1085.3	989.1	3.61	3.29	1237
2	28	1	D_1	0	1.212	1.450	.0035	41.62	6.45	2444.2	.4665	1140.2	—	—	1199.2	826.8	3.99	2.75	2517
2		2	F_1	0	1.219	1.508	.0039	37.35	6.11	2444.2	.4755	1162.2	1345	1.157	1201.6	796.7	4.00	2.65	2615
2	29	1	F_1	0	.846	.960	.0024	60.70	7.79	2444.2	.4324	1056.9	886	.838	906.2	944	3.01	3.14	985
2	30	1	F_1	0	.877	.992	.0024	60.70	7.79	2444.2	.4324	1056.9	898	.850	936.4	944	3.11	3.14	1052

TABLE II.- Concluded

(c) Wings with center of gravity at approximately 58 percent chord

Model	Run	Point	Wing Behavior Left	Wing Behavior Right	M_e	V_e/V_R	ρ_e slugs/cu ft	μ_e	$\sqrt{\mu_e}$	ω_α radians/sec	ω_h/ω_α	ω_h radians/sec	ω_e radians/sec	ω_e/ω_h	V_e ft/sec	V_R ft/sec	$V_e/b_r\omega_\alpha$	$V_R/b_r\omega_\alpha$	q_e lb/ft^2
1	1	1	F_1	F_1	1.333	1.509	0.0034	73.96	8.60	2334.8	0.3403	794.5	1131	1.424	1253.3	830.5	4.364	2.892	2670.3
2	2	1	F_1	F_1	.852	1.099	.0040	62.87	7.93	2553.0	.3510	825.9	905	1.096	883.1	803.4	3.051	2.776	1559.7
3	3	1	F_1	F_1	.950	1.078	.0022	114.31	10.69	2332.0	.3067	715.2	691	.966	1005	932.5	3.504	3.251	1111
3	4	1	F_1	F_1	.875	1.053	.0027	93.14	9.65	2332.0	.3234	754.2	785	1.041	928	881.2	3.235	3.072	1157.4
3	5	1	F_1	F_1	.876	1.078	.0030	83.83	9.16	2332.0	.3313	772.6	823	1.065	924	857.1	3.221	2.988	1280.7
3	6	1	F_1	F_1	.873	1.029	.0025	100.59	10.03	2332.0	.3172	739.7	741	1.002	926	899.8	3.228	3.137	1071.8
3	7	1	F_1	F_1	.936	1.043	.0021	119.75	10.94	2332.0	.3025	705.4	710	1.007	985	944.8	3.434	3.294	1038.6
3	8	1	F_1	F_1	.945	1.049	.0021	119.75	10.94	2332.0	.3025	705.4	704	.998	991	944.8	3.455	3.294	982.1
3	9	1	F_1	0	.962	1.062	.0020	125.74	11.21	2323.0	.2982	692.7	710	1.025	1014	954.6	3.549	3.341	1028.2
3		2	E_1	0	1.179	1.232	.0019	132.36	11.50	2323.0	.2934	681.6	—	—	1193	968.3	4.175	3.389	1352.0
3		3	F_2	0	1.306	1.428	.0024	104.78	10.24	2323.0	.3139	729.2	980	1.344	1290	906.9	4.515	3.174	1996.9
3	10	1	F_1	0	.550	1.067	.0021	119.75	10.94	2323.0	.3025	702.7	704	1.002	1004	941.2	3.514	3.294	1008
3		2	E_1	0	1.223	1.287	.0020	125.74	11.21	2323.0	.2982	692.7	—	—	1228	954.3	4.298	3.340	1508
3		3	F_2	0	1.300	1.400	.0023	109.34	10.46	2323.0	.3103	720.8	968	1.343	1285	917.8	4.497	3.212	1898.9
3	11	1	F_1	0	.931	1.047	.0021	119.75	10.94	2323.0	.3025	702.7	704	1.002	985	941.2	3.447	3.294	1038.1
4	12	1	F_1	F_1	.966	1.059	.0021	119.75	10.94	2374.7	.3025	718.3	766	1.066	1019	962.1	3.489	3.294	1090.3
4		2	E_1	E_1	1.189	1.254	.0021	119.75	10.94	2374.7	.3025	718.3	—	—	1206	962.1	4.129	3.294	1527.2
4		3	[illegible]	F_2	1.268	1.365	.0024	104.78	10.24	2374.7	.3139	745.4	1005	1.248	1265	927.1	4.331	3.174	1920.3
4		4	F_2	F_2	1.269	1.395	.0026	96.72	9.83	2374.7	.3205	761.1	999	1.313	1264	906.2	4.328	3.103	2077
4	13	1	F_1	F_1	.904	1.050	.0025	100.59	10.02	2374.7	.3172	753.3	741	.984	962	916.3	3.294	3.137	1156.8
4	14	1	F_1	F_1	.861	1.013	.0025	100.59	10.03	2374.7	.3172	753.3	729	.968	928	916.3	3.177	3.137	1076.5
4	15	1	F_1	F_1	.853	1.007	.0024	104.78	10.24	2374.7	.3139	745.4	729	.978	934	927.1	3.198	3.174	1066.8
5	16	1	F_1	F_1	.895	1.105	.0024	104.78	10.24	2209.5	.3139	693.6	716	1.032	953	862.6	3.507	3.174	1089.8
5	17	1	F_1	F_1	.928	1.084	.0020	125.74	11.21	2209.5	.2982	658.9	691	1.049	984	907.7	3.621	3.340	968.3
5		2	E_1	E_1	1.201	1.333	.0020	125.74	11.21	2209.5	.2982	658.9	—	—	1210	907.7	4.452	3.340	1464.1
5		3	F_2	F_2	1.272	1.448	.0023	109.34	10.46	2209.5	.3103	685.6	993	1.448	1264	872.9	4.651	3.212	1837.4
5	18	1	F_1	F_1	.871	1.067	.0022	114.31	10.69	2209.5	.3067	677.7	722	1.065	943	883.5	3.470	3.251	978.2

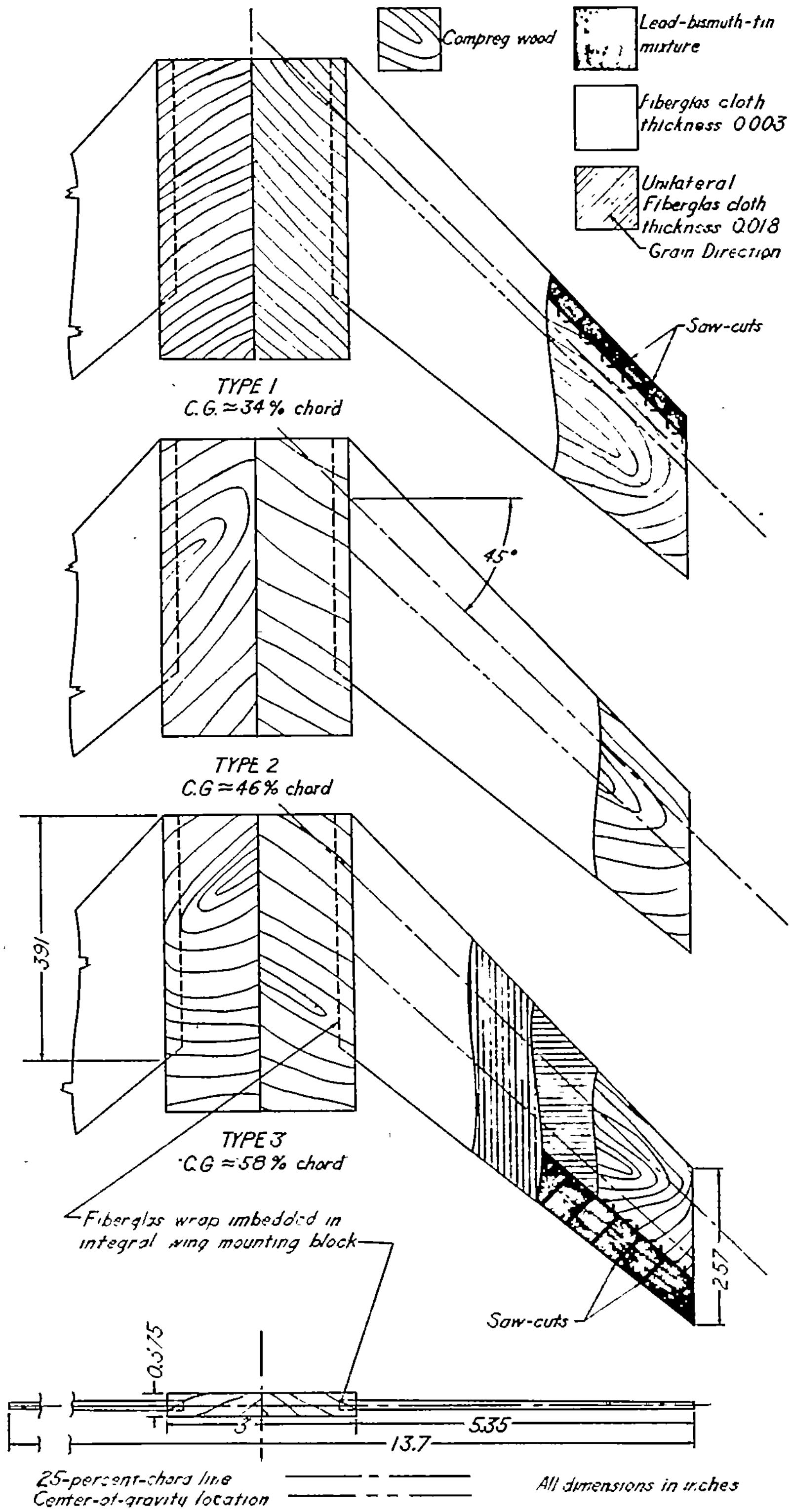

Figure 1.- Cutaway plan-form view of the three types of models showing construction used to vary the center-of-gravity location.

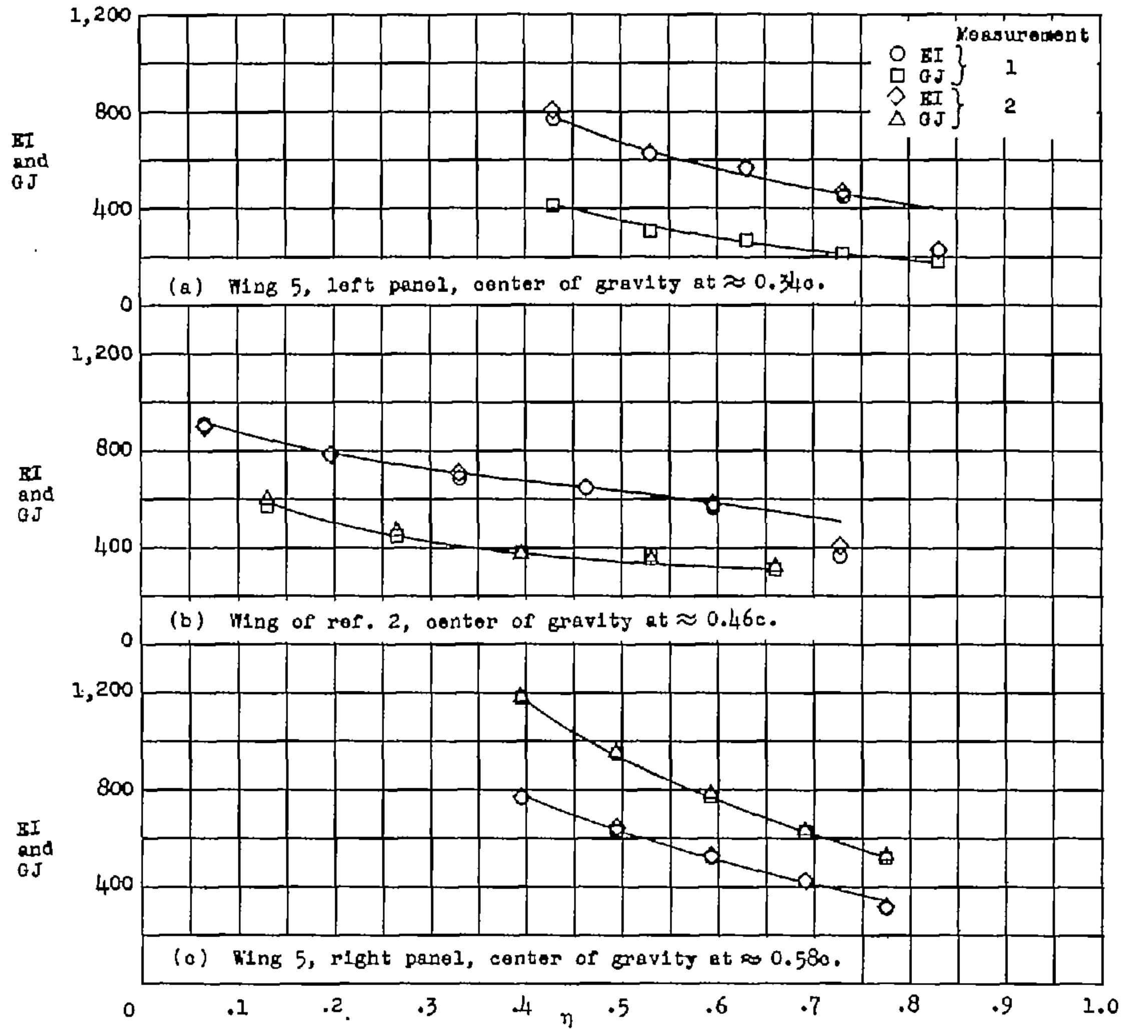

Figure 2.- Typical spanwise stiffness measurements on three models, each having a different center-of-gravity location.

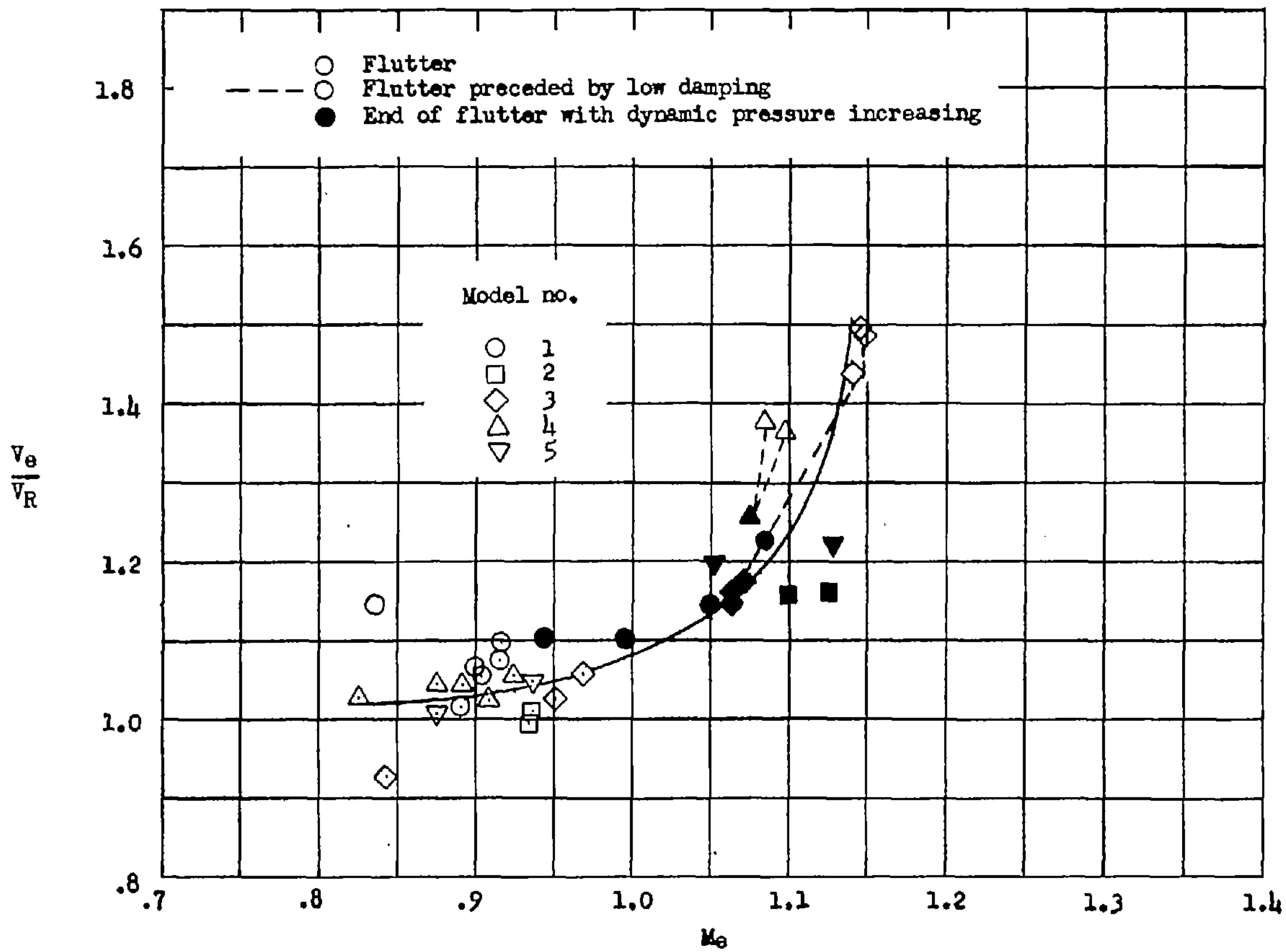

Figure 3.- Variation of flutter-speed ratio with Mach number for models with center-of-gravity locations at approximately 34 percent chord.

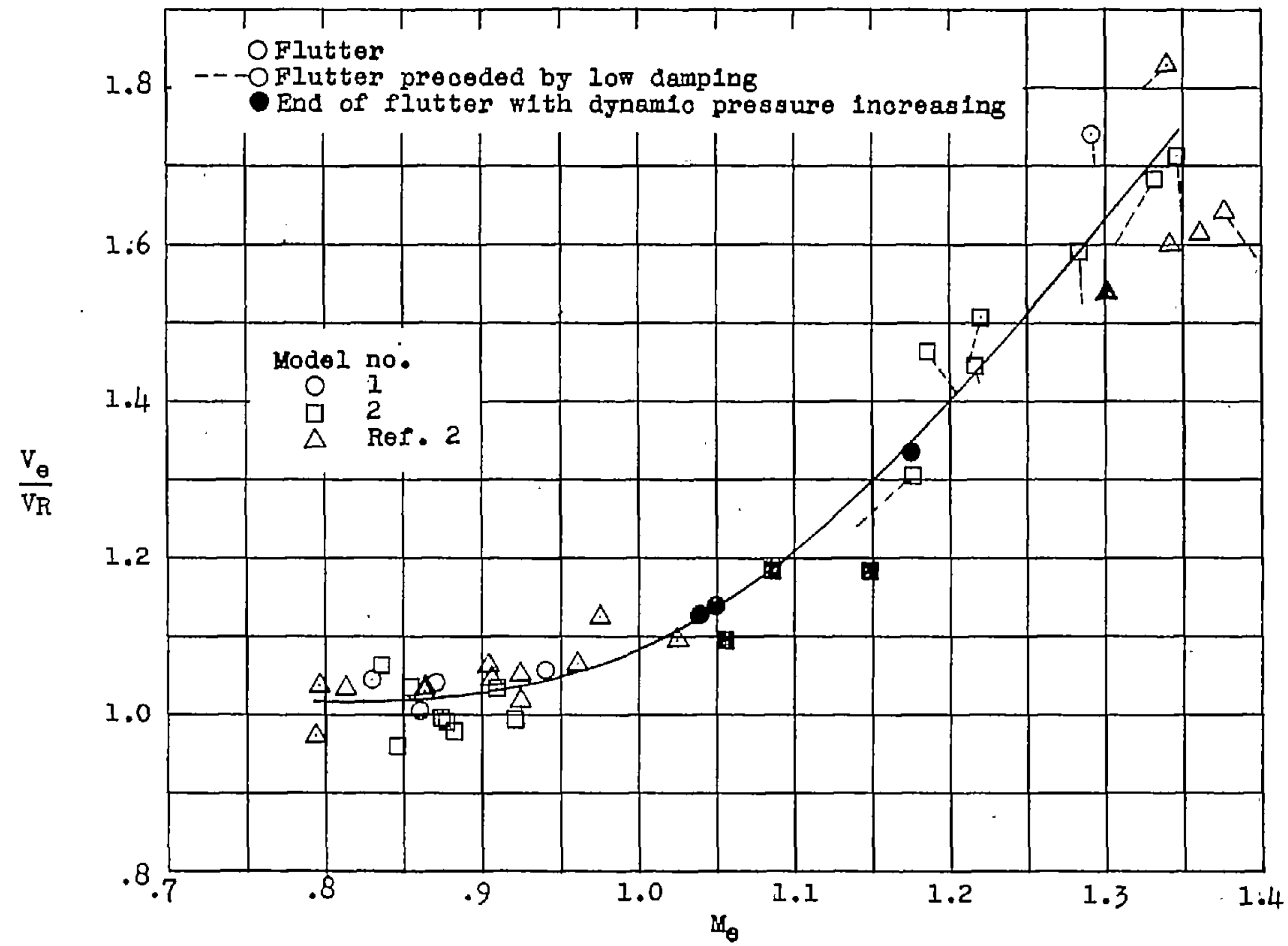

Figure 4.- Variation of flutter-speed ratio with Mach number for models with center-of-gravity locations at approximately 46 percent chord. (Data from ref. 3.)

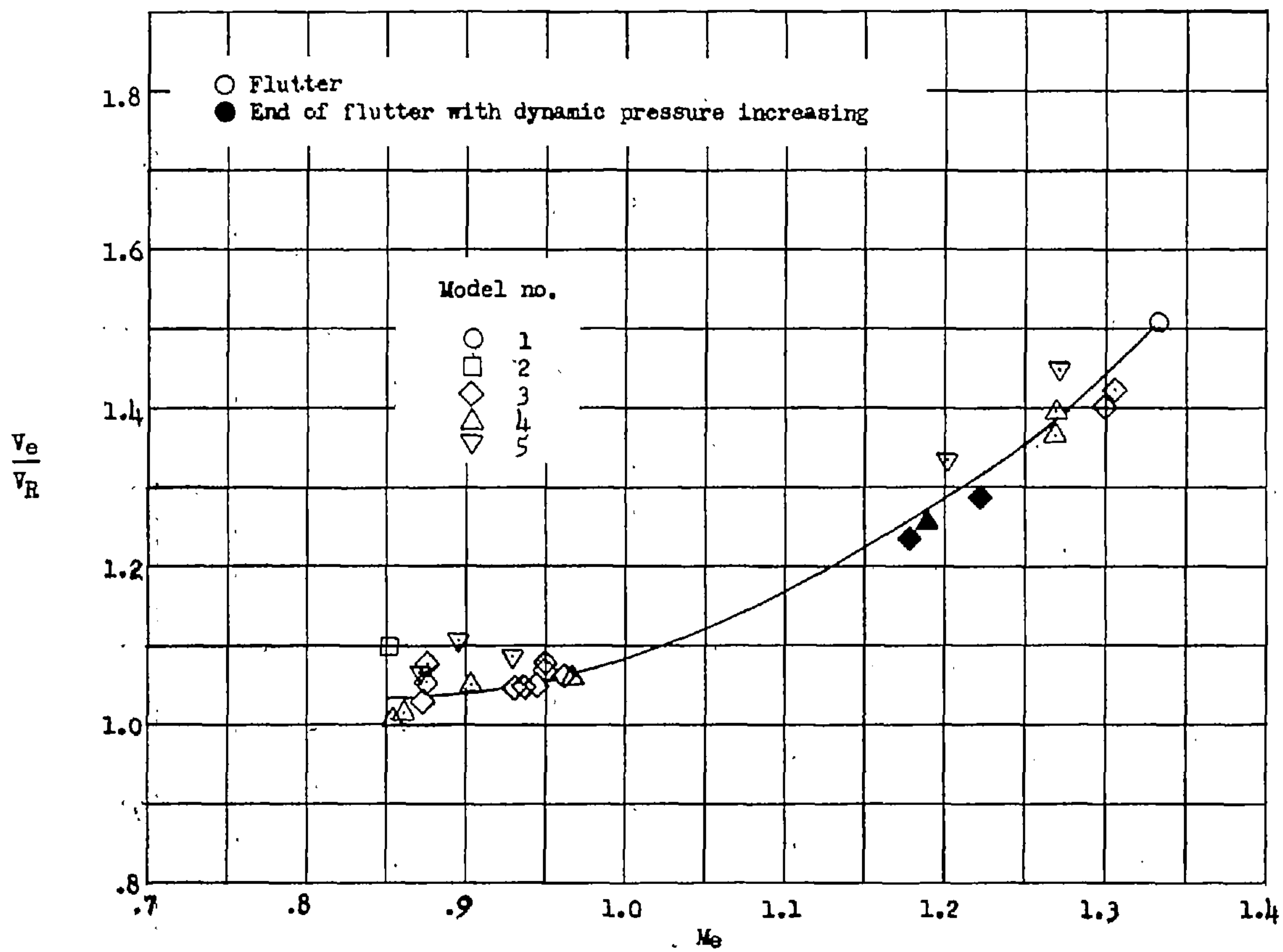

Figure 5.- Variation of flutter-speed ratio with Mach number for models with center-of-gravity locations at approximately 58 percent chord.

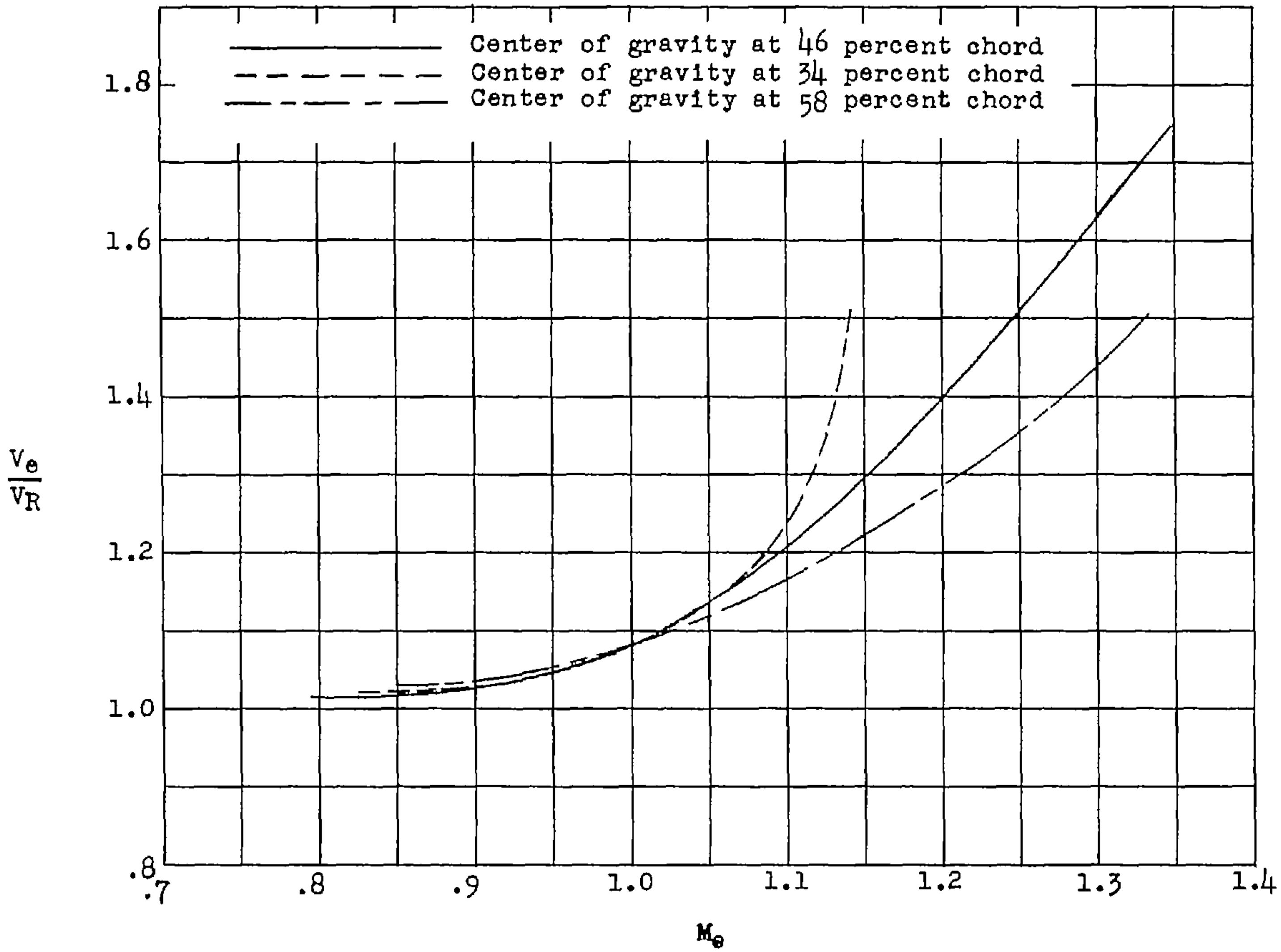

Figure 6.- Effect of center-of-gravity location on the variation of the flutter-speed ratio with Mach number.

NACA - Langley Field, Va.